The $Pr_{0.5}Ca_{0.5}Mn_{1-x}Cr_xO_3$ series ($0 \leq x \leq 0.5$): evidence of steps in the magnetic and transport properties for a narrow composition range

2003 J. Phys.: Condens. Matter 15 2701

(http://iopscience.iop.org/0953-8984/15/17/322)

INSTITUTE OF PHYSICS PUBLISHING JOURNAL OF PHYSICS: CONDENSED MATTER

J. Phys.: Condens. Matter **15** (2003) 2701–2709 PII: S0953-8984(03)58648-9

The $Pr_{0.5}Ca_{0.5}Mn_{1-x}Cr_xO_3$ series ($0 \leqslant x \leqslant 0.5$): evidence of steps in the magnetic and transport properties for a narrow composition range

L Pi, S Hébert[1], C Yaicle, C Martin, A Maignan and B Raveau

Laboratoire CRISMAT, UMR 6508 Associée au CNRS, ISMRA et Université de Caen, 6 Boulevard du Maréchal Juin, 14050 Caen Cedex, France

E-mail: sylvie.hebert@ismra.fr

Received 22 January 2003
Published 22 April 2003
Online at stacks.iop.org/JPhysCM/15/2701

Abstract

The $Pr_{0.5}Ca_{0.5}Mn_{1-x}Cr_xO_3$ series has been investigated up to $x = 0.5$. For low doping content ($x \leqslant 0.04$), the introduction of Cr^{3+} favours the creation of ferromagnetic (FM) regions leading to phase-separation phenomena. Steps in the magnetic and transport properties measured versus field are observed and these properties strongly depend on the thermal history of the samples. For $x = 0.04$–0.06, the samples are almost 100% FM. As the Cr^{3+} concentration increases beyond this optimum doping level of 0.04–0.06, the FM fraction x_{FM} slowly decreases, reflecting the fact that Cr^{3+} is antiferromagnetically coupled to the Mn network, and reaches almost 0 for $x = 0.5$. Beyond the optimum doping, the steps disappear. In a martensitic-like picture, the presence of steps for $x < 0.04$ is consistent with the existence of phase separation. On the other hand, the disappearance of jumps beyond the optimum doping shows that the nature of phase separation, if it exists for $x > 0.04$–0.06, is completely different from the low-x side.

1. Introduction

The half-doped manganite $Pr_{0.5}Ca_{0.5}MnO_3$ has been intensively investigated due to its orbital-ordering and charge-ordering (OO–CO) transition observed at $T_{CO} \approx 250$ K, corresponding to an ordering of the Mn^{3+} and Mn^{4+} species in the CE structure [1]. A magnetic field of 30 T is required to melt this OO–CO state and recover a ferromagnetic (FM) state [2]. Substitution of $Pr_{0.5}Ca_{0.5}MnO_3$ on the Mn site has been shown to be a powerful tool for gradually destroying CO and recovering metal-to-insulator transitions (M/I transitions) as, for example, just 2% of Cr^{3+} is sufficient to induce an insulator-to-metal transition in zero applied field [3]. The $Pr_{0.5}Ca_{0.5}Mn_{1-x}Cr_xO_3$ and $Nd_{0.5}Ca_{0.5}Mn_{1-x}Cr_xO_3$ series have been extensively investigated

[1] Author to whom any correspondence should be addressed.

due to the great efficiency of Cr^{3+} in destabilizing CO/OO, and have been studied in detail as the prototypes of phase-separated systems, with a coexistence of short-ranged OO–CO regions of nanometric scale and FM regions [3–8]. As x increases, FM fractions close to 90% are reached in the case of $Pr_{0.5}Ca_{0.5}Mn_{0.95}Cr_{0.05}O_3$ [9]. The phase-separation phenomena can thus be tuned by increasing the Cr^{3+} content.

Previous studies have shown that, for low doping contents, the magnetic and transport properties of these phase-separated systems present intriguing features. They strongly depend on the thermal history of the samples: for example, the resistivity at 5 K in 0 T can increase by four orders of magnitude upon cycling the sample to room temperature in $Pr_{0.5}Ca_{0.5}Mn_{0.99}Cr_{0.01}O_3$ [10]. More recently, abrupt jumps in the magnetization and resistivity curves measured versus field at low temperature have been observed in $Pr_{0.5}Ca_{0.5}Mn_{1-x}M_xO_3$ samples ($M = Ga^{3+}$, Sn^{4+}) [11].

These two phenomena have been explained in terms of a martensitic-like transition [12, 13]. Because the structural parameters of the OO–CO and FM phases are different [4, 5], strains exist between the two phases. As in martensite, thermal cycling will favour the growth of the OO–CO phase (austenite like) at the expense of the FM one (martensite like). For the $M(H)$ and $\rho(H)$ loops, the role of the magnetic field is to increase the FM region, but the growth of these domains is impeded by the strains. When the magnetic energy is large enough to overcome the elastic one, FM domains can grow in an avalanche-like process.

Steps in the $M(H)$, $\rho(H)$, and $C_p(H)$ curves were first obtained by substituting with the non-magnetic cation Ga^{3+} [11], but similar jumps were observed also in $Pr_{0.5}Ca_{0.5}Mn_{1-x}Ni_xO_3$ [14]. For this series, the maximal FM fraction is close to 40% for $x \sim 0.04$ and jumps are observed whatever x is, below or above this optimum, and persist up to $x = 0.1$, in a region where the thermal cycling effect has disappeared. In the case of Cr^{3+} doping, the FM fraction is much larger, close to 100%, and the possible occurrence of jumps has been investigated to determine the relationship between jumps and phase separation and to check the validity of the martensitic-like scenario.

2. Experimental details

The $Pr_{0.5}Ca_{0.5}Mn_{1-x}Cr_xO_3$ manganites were prepared in the form of polycrystalline samples by mixing the oxides Pr_6O_{11}, CaO, MnO_2, and Cr_2O_3 in stoichiometric proportions as previously described in [3–6].

The purity of the samples was checked by means of x-ray powder diffraction (XRPD) and electron diffraction (ED) microscopy, and their compositional homogeneity was examined by energy-dispersive spectroscopy (EDS) coupled with ED microscopy. The correct composition of the compounds for $0 \leqslant x \leqslant 0.1$ had already been checked [8] and, for $x = 0.5$, a good agreement between the nominal and the actual composition was found, within the limits of accuracy of the technique ($x = \pm 0.01$): the cationic composition $Pr_{0.49}Ca_{0.51}Mn_{0.50}Cr_{0.50}$ was obtained.

The physical properties were measured using a SQUID magnetometer and a VSM for magnetization studies and a Physical Properties Measurements System for the transport measurements (four-probe resistivity), both from Quantum Design.

3. Results

3.1. Structural characterization

For $0 \leqslant x \leqslant 0.5$, the room temperature structure of $Pr_{0.5}Ca_{0.5}Mn_{1-x}Cr_xO_3$ was refined in the *Pnma* space group from XRPD data.

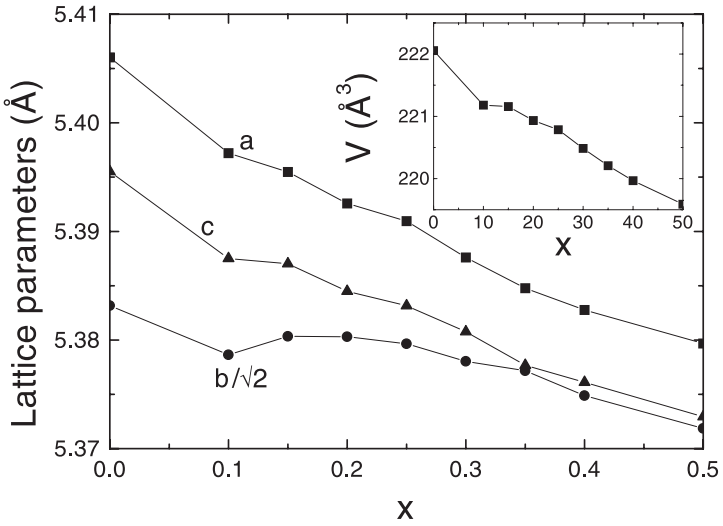

Figure 1. Evolution of the cell parameters and volume (inset) as a function of x.

The lattice parameters versus the substituting content ($0 \leqslant x \leqslant 0.50$) are given in figure 1. The relationship between the cell volume V and the composition x is reported in the inset of figure 1. The Cr-for-Mn substitution leads to a continuous decrease of the volume, in agreement with the smaller size of Cr^{3+} (0.615 Å) compared to Mn^{3+} (0.645 Å). On increasing the Cr content, the distortion of the O′ type, reflecting a cooperative Jahn–Teller effect ($b/\sqrt{2} < c < a$), decreases, in agreement with the non-Jahn–Teller nature of Cr^{3+} (electronic structure $3d^3$).

3.2. Evolution of magnetization and resistivity versus x

Figure 2 summarizes the results previously published [3–6, 8] and extends them to $x = 0.5$. The temperature dependences of the magnetization ($0.005 \leqslant x \leqslant 0.50$) and the resistivity are shown in figures 2(a) and (b) respectively. The influence of Cr doping is spectacular, as ferromagnetism appears early—at the beginning of the doping (see the inset of figure 2(a)). An apparent FM transition around 130 K can be seen as early as $x = 0.015$. With Cr content increasing, the magnetic moment under 1.45 T at 5 K increases rapidly, reaching 3 μ_B for $x = 0.04$. Simultaneously T_c increases to 150 K (for $x = 0.04$). The charge-ordering transition around 250 K shifts to lower temperature and finally vanishes with doping, indicating that the long-range OO–CO ordering has been destroyed by doping. Then T_c and the ferromagnetism begin to decrease as x increases beyond 0.06. In the range of $x > 0.1$, the FM transition is gradually broadened by Cr.

Simultaneously, the resistivity is drastically modified by Cr (see figure 2(b)). Starting from an insulating behaviour for $x \leqslant 0.01$, a metal-to-insulator transition (M/I) is observed as soon as $x = 0.015$ (see the inset of figure 2(b)). Then, a minimum resistivity is obtained for $x = 0.06$, with a M/I transition observed around 135 K, which corresponds to the T_c measured in figure 2(a). As x increases beyond 0.06, the resistivity starts to increase again, and the samples are insulating for $x > 0.2$.

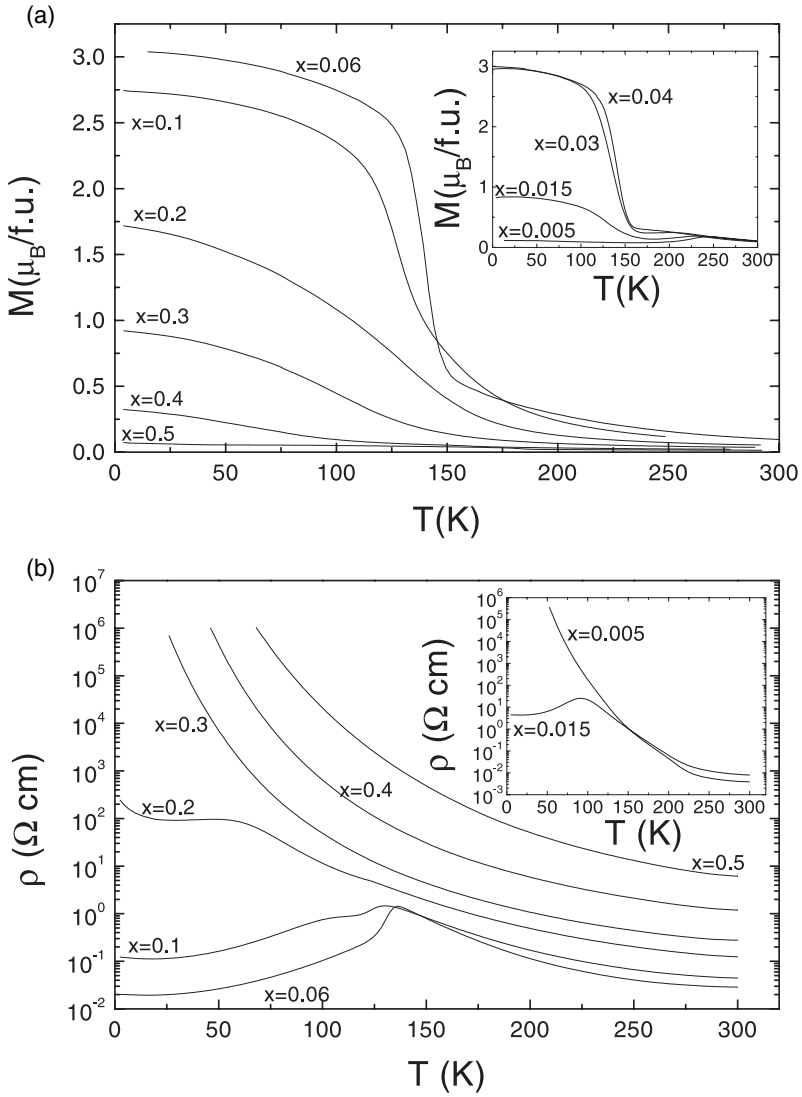

Figure 2. (a) Magnetization measured as a function of T for an applied field of 1.45 T for the $Pr_{0.5}Ca_{0.5}Mn_{1-x}Cr_xO_3$ series ($x > 0.04$, and $x \leqslant 0.04$ in the inset). (b) Resistivity as a function of T measured in 0 T for the same compounds.

3.3. Magnetic coupling between Cr^{3+} and the Mn network

The estimate of the FM fraction induced by Cr^{3+} in $Pr_{0.5}Ca_{0.5}Mn_{1-x}Cr_xO_3$ has been obtained from the $M(H)$ loops measured at $T = 2.5$ K. Following previous studies [15], x_{FM} is defined as M measured under an applied field of 0.25 T, divided by the magnetization of $Pr_{0.5}Ca_{0.5}Mn_{0.95}Ru_{0.05}O_3$ for which a FM fraction of 100% is assumed. The OO/CO phase should not be affected by this moderate field of 0.25 T, while the FM domains are supposed to be aligned [15]. For $Pr_{0.5}Ca_{0.5}Mn_{1-x}Cr_xO_3$, figure 3 shows that x_{FM} reaches a maximum value of 86% for $x = 0.04$–0.06. As more Cr is introduced, x_{FM} slowly decreases and reaches almost zero for $x = 0.5$.

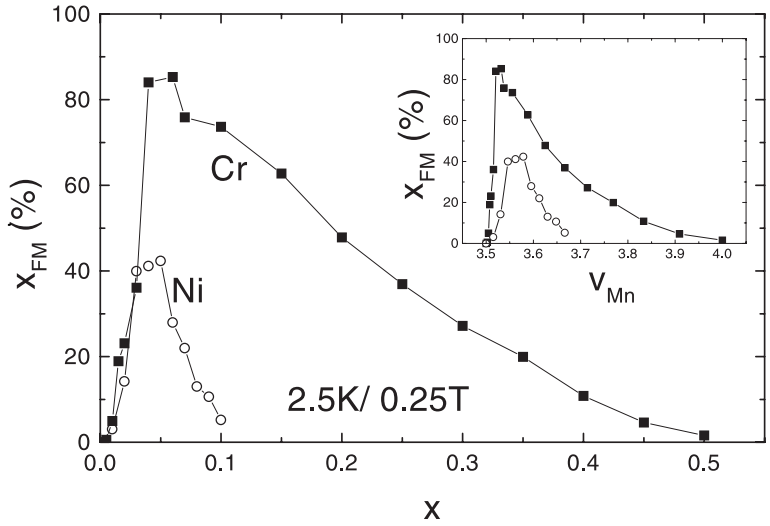

Figure 3. The FM fraction x_{FM} determined at 2.5 K and 0.25 T for the $Pr_{0.5}Ca_{0.5}Mn_{1-x}Cr_xO_3$ and $Pr_{0.5}Ca_{0.5}Mn_{1-x}Ni_xO_3$ compounds. Inset: the same curves plotted as a function of the Mn valence.

Compared to that of other magnetic cations, the efficiency of Cr^{3+} for creating ferromagnetism is greatly enhanced. In figure 3, the results obtained for the substitution of Mn in $Pr_{0.5}Ca_{0.5}Mn_{1-x}M_xO_3$ by M = Cr^{3+} and also Ni^{2+} [14] are presented. As for Cr, the initial increase of x_{FM} with x is very steep for Ni^{2+}, but reaches only 40% for $x \approx 0.05$. Then the Ni efficiency decreases and it has almost completely disappeared for $x = 0.1$, for which $x_{FM} \approx 5\%$. One might argue that the difference between Ni and Cr is related to the fact that the Mn valence is larger in $Pr_{0.5}Ca_{0.5}Mn_{1-x}Ni_xO_3$ than in $Pr_{0.5}Ca_{0.5}Mn_{1-x}Cr_xO_3$ for a given x, as Ni is divalent and Cr is trivalent [16]. However, when x_{FM} is plotted as a function of the calculated Mn valence v_{Mn} (see the inset of figure 3), the two curves are still not superimposed and the efficiency of Cr^{3+} is still much larger than that of Ni^{2+}.

It had been previously proposed that Cr^{3+} replaces Mn^{3+} with the opposite spin direction for $x \leqslant 0.3$ [16, 17]. Figure 4 presents the magnetization measured at 5 K and 5 T as a function of x. For $x \geqslant 0.04$, M decreases as a function of x and follows the law $M(x) = 3.5 - 7x$ up to $x = 0.5$, characteristic of $Pr_{0.5}Ca_{0.5}Mn^{4+}_{0.5}Mn^{3+}_{0.5-x}Cr^{3+}_xO_3$ when the Mn^{3+} and Mn^{4+} are ferromagnetically coupled and Cr^{3+} is AFM coupled to Mn [6]. For $x = 0.5$, only Mn^{4+}–Cr^{3+} antiferromagnetic superexchange interactions exist. The inset of figure 4 reflects the evolution of this series from FM behaviour for x close to 0.04–0.06 to antiferromagnetism: the inset of figure 4 shows the evolution of the inverse of susceptibility χ^{-1} versus T. For high temperature, $\chi^{-1}(T)$ is linear and $\chi(T)$ follows a Curie–Weiss law with θ_p changing from a positive value close to +170 K for $x = 0.06$ to a negative value close to −90 K for $x = 0.5$. Note that for x up to 0.06, θ_p keeps a rather fixed value, close to +170 K, indicating that the Mn^{3+}/Mn^{4+} FM double exchange (DE) is dominating. In contrast, for $x \geqslant 0.1$, θ_p decreases, which shows that the antiferromagnetic interactions start to overcome the DE FM ones.

3.4. Steps in magnetic and transport properties

In figure 5(a), the M–H loops at 2.5 K are presented for $x = 0.015$. As in the case of $Pr_{0.5}Ca_{0.5}Mn_{1-x}M_xO_3$ with M = Ga^{3+}, Mg^{2+}, Ni^{2+}, Co^{2+}, ..., the M–H loops show steps

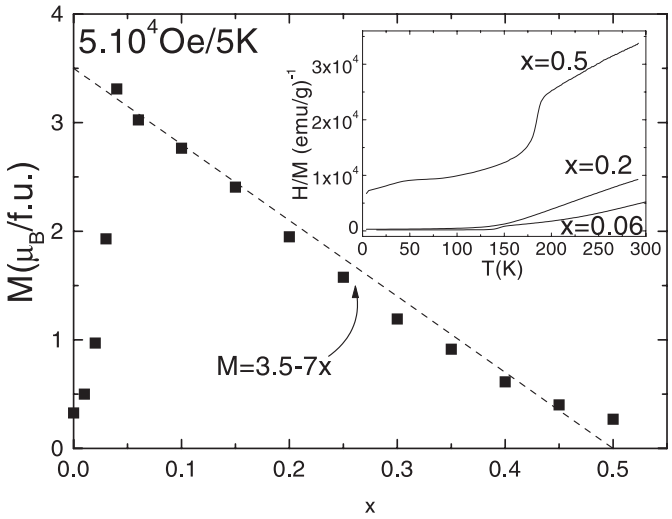

Figure 4. M as a function of x measured at 5 K and 5 T. The dotted line is $M = 3.5 - 7x$, which corresponds to the evolution of M when Mn^{3+} and Mn^{4+} are FM coupled and Cr^{3+} is AFM coupled to Mn^{3+}/Mn^{4+}. Inset: $1/\chi(T)$ curves measured under 1.45 T for $x = 0.06$, 0.2, and 0.5.

for the field-increasing branch. The corresponding magnetic fields are 2.5 and 4 T. Similar jumps in $M(H)$ are observed for $x < 0.04$. The height of the jumps is always in the range 0.1–0.5 μ_B, similar to what is observed for $Pr_{0.5}Ca_{0.5}Mn_{1-x}Ni_xO_3$ [14], and they disappear at $T = 5$ K. Jumps are also observed on the increasing loop of the $\rho(H)$ curves for $x < 0.04$, as shown in figure 5(b).

The thermal cycling effect as previously observed in [10, 12, 14] is evidenced in figure 6 for $x = 0.01$. At 2.5 K, M decreases over the whole field range after the sample has been warmed to room temperature, and the position of the steps is shifted to larger magnetic fields (from 2.5 T for the first loop, to 4.25 T for the second loop) after cycling.

Figure 7 presents the results obtained for $x > 0.03$. For $x = 0.04$, the $M(H)$ curve is characteristic of a ferromagnet, with M rapidly increasing to its saturation value. As x increases further (for example, $x = 0.3$ in figure 7), M at high field decreases, while the remanent magnetization increases but no jumps are observed. Note that for $x = 0.04$, three $M(H)$ loops have been measured with the sample warmed to 300 K between loop recordings. The three loops are superimposed; the thermal cycling effect has disappeared.

4. Discussion and concluding remarks

From figure 3 it can be seen that the x_{FM}-curve has a peak at $x = 0.04$–0.06. This peak divides the Cr-doped compounds into two families. On the left, the ferromagnetism in the Cr-doped system is increasing with the doping. Magnetic and resistivity measurements show steps and a thermal cycling effect. On the right, beyond the optimum doping, the ferromagnetism is weakened by substitution, and the steps and thermal cycling effect disappear.

A model for describing the evolution of x_{FM} with x for small x was previously proposed [17]. Charge-ordered $Pr_{0.5}Ca_{0.5}MnO_3$ is a CE-type oxide, which consists of FM zigzag chains of Mn^{3+}/Mn^{4+} cations, the coupling between chains being antiferromagnetic. As was explained before [17], one Cr^{3+} substitutes for one Mn^{3+} for charge reasons and is antiferromagnetically coupled with all its nearest neighbours. The spins of Mn^{3+} and Mn^{4+}

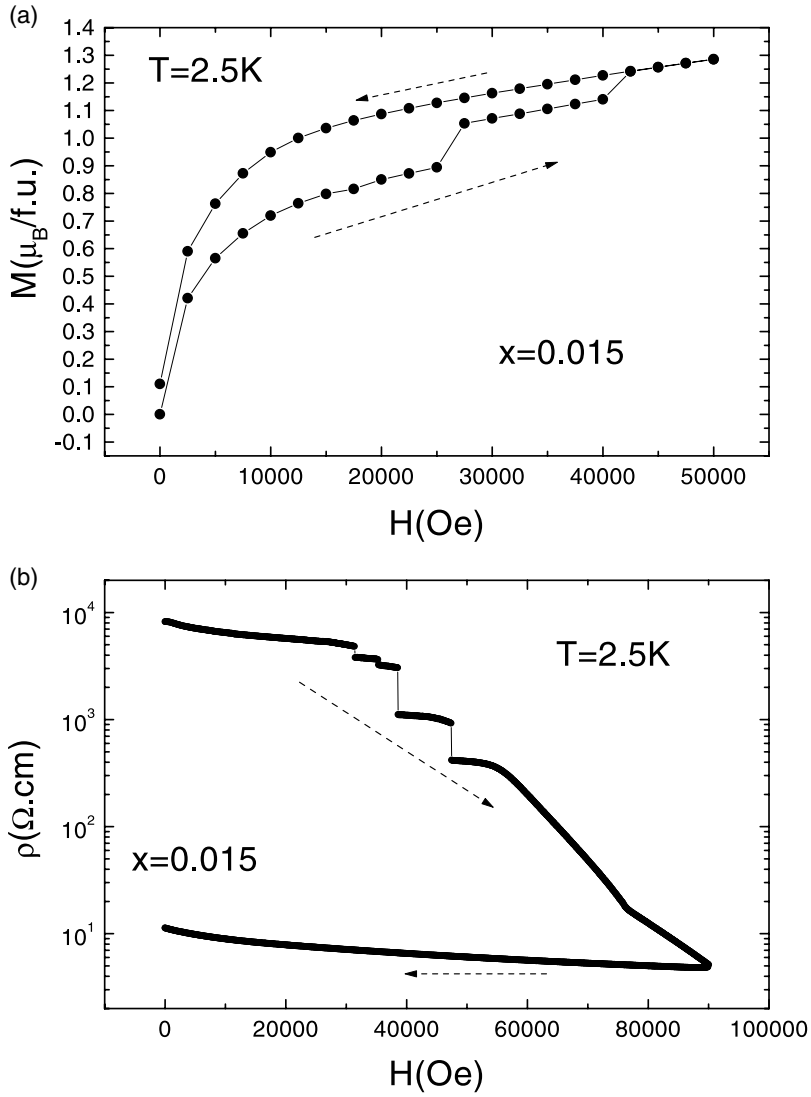

Figure 5. $M(H)$ (a) and $\rho(H)$ (b) curves for $Pr_{0.5}Ca_{0.5}Mn_{0.985}Cr_{0.015}O_3$ measured at $T = 2.5$ K.

in the FM zigzag chain will be reversed while the spins in the nearest chains are unchanged, as the coupling was already antiferromagnetic. The three chains will thus be ferromagnetically coupled around the Cr^{3+} ion. Hence by a 'domino' effect, the Cr^{3+} ions can create elliptical FM microregions around them in the OO–CO phase. This explains the appearance of ferromagnetism and phase separation in the low-doping range. When the FM fraction reaches the percolation threshold, the M/I transition appears.

When more and more Cr^{3+} cations are introduced, the antiferromagnetic coupling between Cr^{3+} and Cr^{3+}, Cr^{3+} and Mn^{4+}, Mn^{4+} and Mn^{4+} should be taken into account. According to Goodenough's work [18], two cations with empty e_g orbitals are expected to establish a weak antiferromagnetic superexchange interaction. With many Cr^{3+} in the matrix, the number of

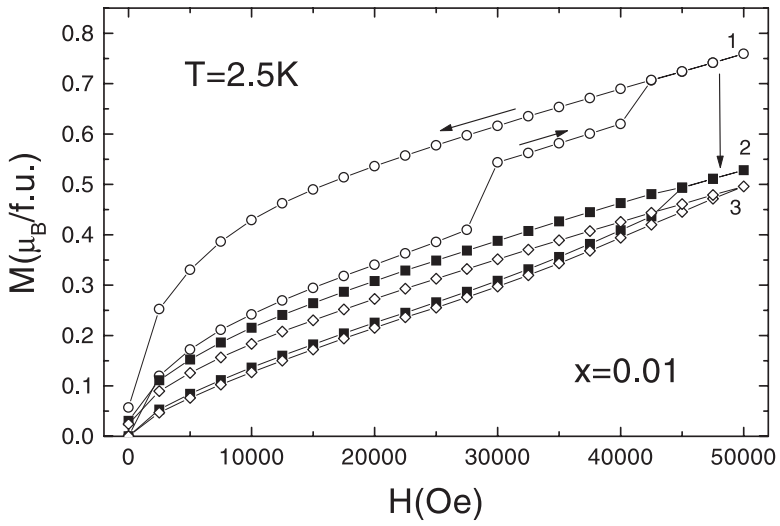

Figure 6. Three successive $M(H)$ curves for $Pr_{0.5}Ca_{0.5}Mn_{0.99}Cr_{0.01}O_3$ measured at $T = 2.5$ K. The sample was systematically warmed to 300 K between curve recordings and zero-field cooled to 2.5 K.

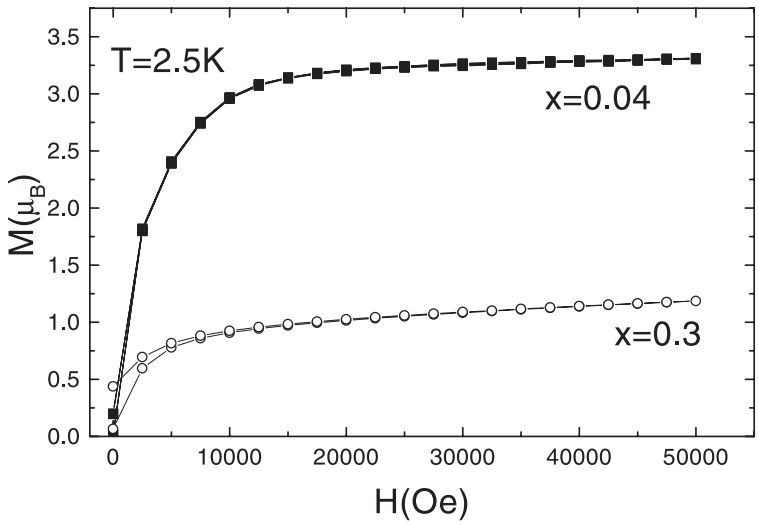

Figure 7. $M(H)$ loops at $T = 2.5$ K for $Pr_{0.5}Ca_{0.5}Mn_{0.96}Cr_{0.04}O_3$ and $Pr_{0.5}Ca_{0.5}Mn_{0.7}Cr_{0.3}O_3$.

Mn^{3+} ions is noticeably reduced. Antiferromagnetic interactions between Cr^{3+} and Mn^{4+} ions can occur and the FM DE interaction between Mn^{3+} and Mn^{4+} is weakened. Therefore, the antiferromagnetism in the matrix begins to be reinforced and the FM fraction is decreased. As a consequence, the resistivity increases with Cr^{3+} for Mn^{3+} substitution for low T. At high T, the increase of resistivity as the Cr^{3+} content increases is linked to the effect of scattering by impurities.

Below $x = 0.06$, the jumps observed in the magnetic and transport properties can thus be consistently explained in the martensitic-like scenario. For low doping concentration, phase separation exists and jumps occur. They are similar to the ones measured for

$Pr_{0.5}Ca_{0.5}Mn_{1-x}M_xO_3$ with M = Ga^{3+}, Mg^{2+}, Ni^{2+}, Co^{2+}, ... [11, 14]. As for $Pr_{0.5}Ca_{0.5}Mn_{1-x}NiO_3$, they still exist when the FM fraction is large, close to 40%, for $x = 0.03$ [14]. Above this content, the influence of Cr^{3+} is drastic and the FM fraction has already reached almost 90% when $x = 0.04$ (figure 3). For such a large x_{FM}, jumps disappear, supporting the idea that they are mainly related to the nucleation of a FM phase embedded in an OO–CO matrix, and impeded by the strains between the two regions.

Above $x = 0.04$–0.06, x_{FM} decreases again, but the situation is completely different from the left side of the $x_{FM}(x)$ curve. On the right, the increase of Cr^{3+} content gradually dilutes the FM DE interactions between Mn^{3+} and Mn^{4+}, and increases the AFM coupling with Mn^{4+}. As x increases, x_{FM} decreases but no jumps are observed, even when x_{FM} again reaches 40% or less (for $x > 0.25$), i.e. the fraction below which jumps are observed on the left of the $x_{FM}(x)$ curve. The value of x_{FM} is thus not the only parameter which governs the existence of jumps. The way in which the Cr^{3+} reduces the FM interactions and reinforces the AFM has been investigated only by macroscopic techniques (i.e. via magnetization), and microscopic details are still lacking, but the absence of jumps shows that phase separation, if it exists for $x > 0.04$, is most probably completely different from that for low x-content.

Considering the $x_{FM}(x)$ curve and its relationship with jumps, the situation is thus very different from that for $Pr_{0.5}Ca_{0.5}Mn_{1-x}Ni_xO_3$, for which jumps are observed even for the largest x-value investigated—equal to 0.1, i.e. for x below or above the optimum of x_{FM}. The major difference between the cases for Ni^{2+} and Cr^{3+} is that, with Ni^{2+}, x_{FM} never reaches 90% but is limited to 40%. The way in which x_{FM} decreases with x beyond its optimum is thus completely different from the case for Cr^{3+}, and the phase separation in $Pr_{0.5}Ca_{0.5}Mn_{1-x}Ni_xO_3$ is most probably never completely suppressed up to $x = 0.1$, as proposed in [14]. A neutron diffraction study performed at low T on these samples would definitely confirm the validity of this assumption.

References

[1] Wollan E O and Koehler W C 1955 *Phys. Rev.* **100** 545
[2] Tokunaga M, Miura N, Tomioka Y and Tokura Y 1998 *Phys. Rev.* B **57** 5259
[3] Raveau B, Maignan A and Martin C 1997 *J. Solid State Chem.* **130** 162
[4] Damay F, Martin C, Maignan A, Hervieu M, Raveau B, Bourée F and André G 1998 *Appl. Phys. Lett.* **73** 3772
[5] Martin C, Maignan A, Damay F, Hervieu M, Raveau B, Jirak Z, André G and Bourée F 1999 *J. Magn. Magn. Mater.* **202** 11
[6] Mahendiran R, Hervieu M, Maignan A, Martin C and Raveau B 2000 *Solid State Commun.* **114** 429
[7] Katsufuji T, Cheong S-W, Mori S and Chen C-H 1999 *J. Phys. Soc. Japan* **68** 1090
[8] Hervieu M, Martin C, Barnabé A, Maignan A, Mahendiran R and Hardy V 2001 *Solid State Sci.* **3** 391
[9] Hébert S, Maignan A, Martin C and Raveau B 2002 *Solid State Commun.* **121** 229
[10] Mahendiran R, Maignan A, Hervieu M, Martin C and Raveau B 2001 *J. Solid State Chem.* **160** 1
[11] Hébert S, Hardy V, Maignan A, Mahendiran R, Hervieu M, Martin C and Raveau B 2002 *J. Solid State Chem.* **165** 6
[12] Mahendiran R, Maignan A, Hervieu M, Martin C and Raveau B 2001 *J. Appl. Phys.* **90** 2422
[13] Hardy V, Hébert S, Maignan A, Martin C, Hervieu M and Raveau B 2003 *J. Magn. Magn. Mater.* submitted
[14] Hébert S, Maignan A, Hardy V, Martin C, Hervieu M, Raveau B, Mahendiran R and Schiffer P 2002 *Eur. Phys. J.* B **29** 419
[15] Kim K H, Uehara M, Hess C, Sarma P A and Cheong S W 2000 *Phys. Rev. Lett.* **84** 2961
[16] Toulemonde O, Studer F, Barnabé A, Raveau B and Goedkoop J B 1999 *J. Appl. Phys.* **86** 2616
Studer F, Toulemonde O, Goedkoop J, Barnabé A and Raveau B 1999 *Japan. J. Appl. Phys.* **38** 377
[17] Martin C, Maignan A, Hervieu M, Autret C, Raveau B and Khomskii D I 2001 *Phys. Rev.* B **63** 174402
[18] Goodenough J B, Wold A, Arnott R J and Menyuk N 1961 *Phys. Rev.* **124** 373